THE ASTROPHYSICAL JOURNAL, 429:L9–L12, 1994 July 1

CONSPICUOUS TANGENTIAL ALIGNMENT OF FAINT BLUE AND RED OBJECTS IN CLUSTER 0024+1654[1]

AGGELIKI KASSIOLA, ISRAEL KOVNER, BERNARD FORT, AND YANNICK MELLIER
Observatoire Midi-Pyrénées, 14 av. E. Belin, Toulouse 31400, France
Received 1994 February 22; accepted 1994 April 12

ABSTRACT

We report a study of correlation between color $B-I_{7800}$ and tangential alignment caused by gravitational distortion of faint objects in Cl 0024+1654. Along with the better known gravitational distortion of blue background galaxies, we find a highly significant alignment of red objects with color in a very narrow range, $2.7 \leq B-I \leq 2.8$. The objects responsible for this red alignment signal can be elliptical galaxies belonging to a cluster at redshift $z_r \lesssim 1.8$. A speculative possibility is that these objects are primordial galaxies at $z_r = 5.5$ and Lyα active.

Remarkably, Cl 0024+1654 plays a role of an optical attachment to a man-made telescope which enables us to detect members of a very distant cluster of galaxies statistically, by their color and tangential alignment. The method described here is very simple and can be routinely used to investigate galaxy clustering in the early universe.

Subject headings: gravitational lensing — galaxies: clusters of — galaxies: general — methods: statistical

1. INTRODUCTION

In a previous paper (Kassiola, Kovner, & Fort 1992, hereafter Paper I) we presented CFHT observations of the cluster 0024+1654 ($z = 0.39$) with unique seeing (0".5 with I_{7800} filter and 0".7 with B filter), sampling (1 pixel = 0".206), and depth (180 m in B and 165 m in I). Apart from the blue giant triple arc discussed in Paper I, these images contain other blue and red possible gravitational lensing features.

The blue arclets are well known (e.g., Fort 1992), and we expected that color selection for bluer objects can enhance the signal-to-noise ratio in statistical studies of gravitational fields of clusters based on distortions of background objects.

Red arcs and arclets, although known in some clusters of galaxies (e.g., A2218, Pelló et al. 1992), are relatively less studied than the blue ones, because the observed clusters themselves tend to be red. However, we noticed that there is a red "color window" between the typical colors of elliptical galaxies, $B-I \sim 3.0$–3.5, and those of spirals, $B-I \sim 1.5$–2.5, in Cl 0024−1654, and we wondered whether this window can be used in searches for background galaxies distorted by lensing.

To investigate the color-lensing correlation, we measured the tangential alignment of faint objects in Cl 0024+1654 as a function of the $B-I$ color. In addition to the expected large "alignment signal" in blue objects, we discovered a highly significant alignment of red objects with color in a very narrow range: $2.7 \leq B-I \leq 2.8$.

We give an account of the statistics of the tangential alignment in § 2, address the color and redshift of the objects responsible for the "red signal" in § 3, and summarize in § 4.

2. TANGENTIAL ALIGNMENT

A direct gravitational lensing method to select statistically for objects that are behind a cluster of galaxies is to examine their shapes and orientations. The analysis of correlations between the shapes of background objects and their positions with respect to possible lenses was pioneered by Tyson et al. (1984) who measured shape parameters by means of the FOCAS package (Jarvis & Tyson 1981; Valdes, Tyson, & Jarvis 1983). Webster (1985) pointed out that this technique can be particularly useful in detection of gravitational lensing by clusters of galaxies. References to recent literature on the subject can be found in Blandford & Narayan (1992) or Schneider, Ehlers, & Falco (1992).

We applied the recent version of FOCAS to the B and I images of Cl 0024+1654 and obtained a catalog of 1180 objects with $B < 28$ mag and $I < 26$ mag. These objects and their properties (including their I magnitude) were defined by B isophotes at a 3 σ level of the sky background.[2] For each object the catalog contains coordinates of the center of light $\boldsymbol{c} = (c_x, c_y)$, area A, and magnitudes B and I within the B-isophote, central brightness μ_0^B defined in a $3px \times 3px$ square centered at $\boldsymbol{c}$, and elements $[S_{xx}, S_{yy}, S_{xy}]$ of the matrix of the second moment of the light distribution. We parameterize this matrix as

$$S = \text{const} \times \left[\hat{I} + \epsilon \begin{pmatrix} \cos 2\phi & \sin 2\phi \\ \sin 2\phi & -\cos 2\phi \end{pmatrix}\right], \qquad (2.1)$$

where $\hat{I}$ is the unit matrix, and $\epsilon \geq 0$. Although the objects have arbitrary shape, we use an analogy to ellipses and regard ϕ as the declination of a major axis.

For each object, we calculate an "axis-to-tangent" angle η as follows. We assume the cluster center at the center of light of the four large central ellipticals grouped together, at coordinates $\boldsymbol{C} = (595,509)$ in pixels. We take a circle centered at the cluster center and a tangent to this circle, both passing through the center of light of the object. We then set η equal to the angle between this tangent and the major axis of the object.

Our statistics is based on the average $\bar{\eta}$ ("the alignment signal") calculated for groups of objects selected from the catalog by criteria discussed below. To appreciate the significance of the signal we calculate $P_N(<\bar{\eta})$, the probability for an

[1] Based on observations at the Canada-France-Hawaii Telescope (CFHT).

[2] Despite the slightly better seeing in the I image, the B image is deeper, because of an exceptional quantum efficiency ($\eta^B \approx 90\%$ whereas $\eta^I \approx 40\%$), and a lower sky background.

average smaller than that obtained to occur in a sample of the same number of objects with a uniform distribution of orientations (for which the expectation is $\bar{\eta} = 45°$). For $N \leq 40$ we use the precise formula

$$P_N(<\bar{\eta}) = \sum_{0 \leq j < 2\bar{\eta}N/\pi} \frac{(-1)^j}{j!(N-j)!} \left(\frac{2\bar{\eta}N}{\pi} - j\right)^N , \qquad (2.2)$$

and for $N > 40$ we use the approximation by a normal distribution

$$P(<\bar{\eta}) \approx \frac{1}{2}\left\{1 - \mathrm{erf}\left[\left(\frac{1}{2} - \frac{2\bar{\eta}}{\pi}\right)\sqrt{6N}\right]\right\} , \qquad (2.3)$$

where erf is the error function. These formulae can be easily derived by standard methods (see, e.g., Kendall & Stuart 1977).

The noise in $\bar{\eta}$ comes from the intrinsic shapes and orientations of galaxies, from the finite seeing, pixelization, and background, and from contamination by foreground galaxies of which many belong to the cluster.[3] Apart from color differentiation, we want selection rules which would filter out some of this noise. The background is addressed by FOCAS when we define objects by 3 σ isophotes. We reduce the seeing and pixelization noise by selecting objects with areas larger than some threshold. Selection against foreground contamination can be done by setting a threshold on either the magnitude, or the average brightness, or the central brightness of the objects. As one of us did earlier (in cluster A370, B. Fort, unpublished), we find that selection for faint central brightness μ_0^B is the best of these options.

Next, we differentiate the objects by color and plot histograms of N, $\bar{\eta}$ and $P(<\bar{\eta})$ versus $B-I$ in Figure 1, for two values of histogram steps, and thresholds $A \geq 14$ pixels and $\mu_0^B \geq 24.5$ mag $(")^{-2}$. The alignment signals are best seen in the histogram of significance, $P(<\bar{\eta})$. There are clear and strong signals in two color ranges, a "blue" signal that is relatively wide in color, $0.8 \lesssim B-I \lesssim 1.3$, and a very narrow in color "red" signal, $2.7 \leq B-I \leq 2.8$. The dependence of the significance on the thresholds in area A and in central brightness μ_0^B is shown in Figure 2, for the "all colors" signal (no color selection), for the "blue" signal, and for the "red" signal.

The larger significance of the "blue" signal as compared to the "all colors" signal is not surprising, given the common experience of having many blue arclets in predominantly red clusters. In practice, selection for bluer color can be used for enhancing the gravitational distortion signal in clusters. This suggestion has already been tried on the overlap of the B and V fields of Cl 0024+1654 and its vicinity, reported by Bonnet et al. (1994), and the signal-to-noise ratio was indeed increased (H. Bonnet 1994, private communication).

The red spike of alignment in Figure 1 has $N = 23, \bar{\eta} \approx 20°.4$, and $P_{23}(<20°.4) \approx 10^{-6}$. If the assumed center were shifted by $\leq 10''$, the values of $\bar{\eta}$ and of $\log_{10} P_{23}(<\bar{\eta})$ would change by $\lesssim 7\%$ and $\lesssim 11\%$, respectively. In Figure 2 we see that a different choice of thresholds could reduce the significance of the red signal to $\sim 10^{-4.5}$. The photometry errors of FOCAS are not available at this time, however the red spike would not be so narrow if these errors were larger than ~ 0.05 mag. In what follows we shall assume that the red spike is real.

3. OBJECTS RESPONSIBLE FOR THE RED SIGNAL

The 23 objects involved in the red spike of alignment are marked in Figure 3 (Plate L2), and their properties determined by FOCAS are listed in Table 1. Some of them can be foreground contamination, and some are truly background objects which we shall call "Tangentially Aligned Red

[3] We neglect the atmospheric refraction and tracking errors: these systematic effects have been important for the objects considered by Bonnet, Mellier, & Fort (1994), which are $\gtrsim 1$–2 mag fainter than the ones we consider here.

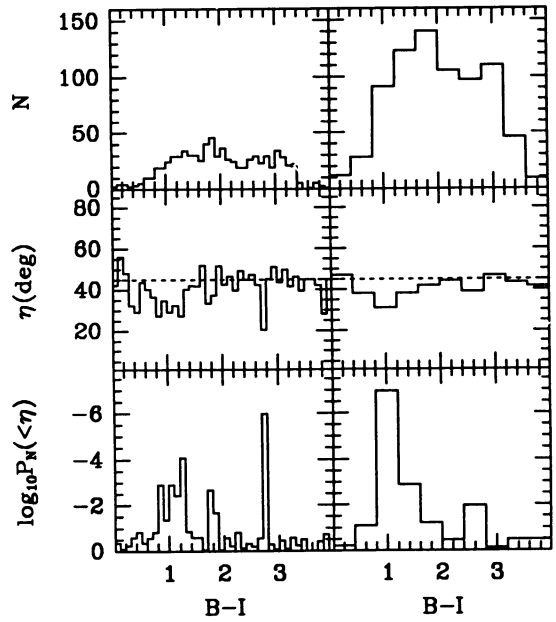

FIG. 1.—Left-hand panels show, from top to bottom, histograms of the number of objects per bin, of the average axis-to-tangent angle per bin, and of the probability to have the average smaller than that found, vs. $B-I$, for bin $\Delta(B-I) = 0.1$ mag, for thresholds $A \geq 14$ pixels and $\mu_0^B \geq 24.5$ mag. The right-hand panels show the same with bin 0.4 mag.

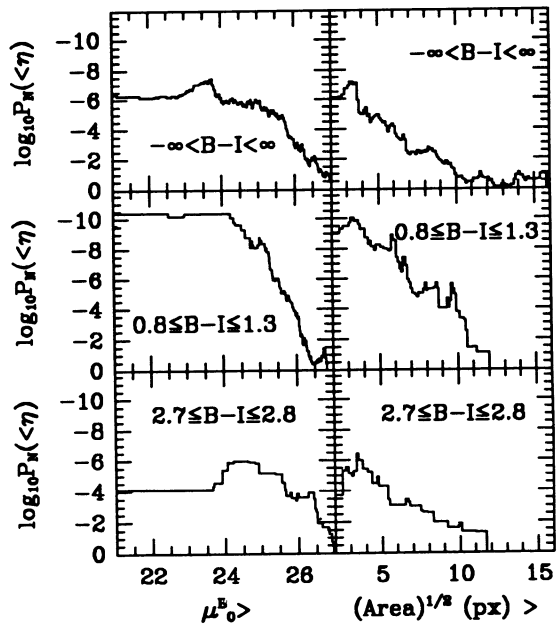

FIG. 2.—Dependence of significance on thresholds in central brightness μ_0^B (*left*, for $A \geq 14$ pixels) and area A (*right*, for $\mu_0^B \geq 24.5$), for "all colors" (*top*), "blue" (*middle*), and "red" (*bottom*) signals.

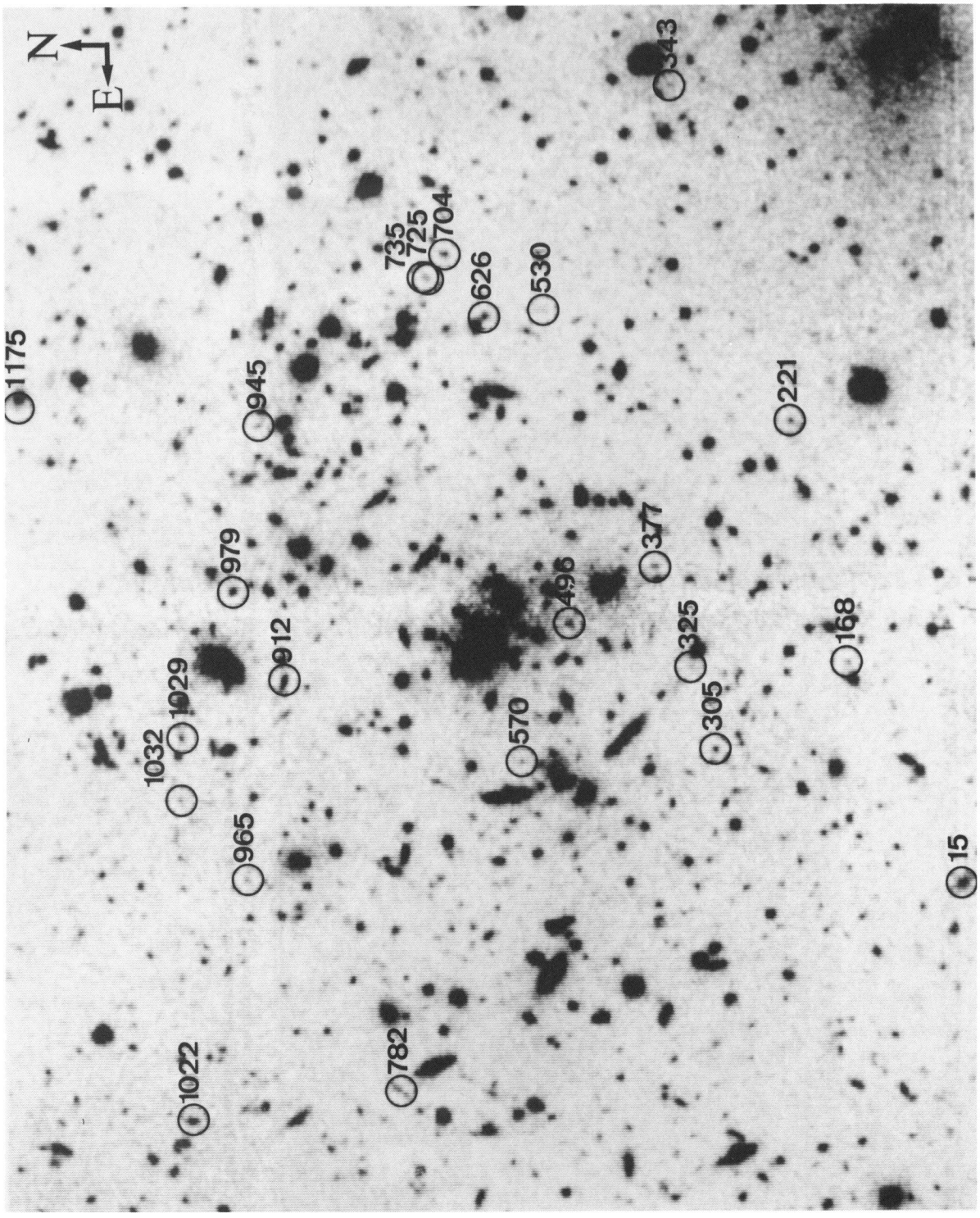

FIG. 3.—*B* image of the cluster Cl 0024+1654. The 23 objects with color $2.7 \leq B-I \leq 2.8$ are indicated by circles drawn around them. The picture dimensions are 1250×1000 pixels, and the scale is 1 pixel = 0".206.

TABLE 1

THE 23 OBJECTS OF COLOR $2.7 \leq B-I \leq 2.8$

Name	c_x	c_y	B	$B-I$	μ_0^B	Area	ϵ	ϕ	η
15	338.2	29.6	23.66	2.72	24.68	120	0.24	−58.2	28.2
168	564.3	142.4	26.59	2.73	26.45	29	0.20	−8.8	1.6
221	811.4	196.0	25.14	2.78	25.55	68	0.15	30.9	2.6
305	476.8	276.6	25.55	2.77	25.62	56	0.02	−18.9	11.9
325	560.9	300.0	27.47	2.76	27.03	22	0.29	45.0	58.8
343	1157.4	313.2	27.03	2.79	26.82	29	0.47	84.3	13.1
377	663.1	334.7	25.89	2.73	26.26	55	0.67	62.1	44.3
496	606.9	422.0	25.22	2.76	25.79	98	0.31	−36.0	33.7
530	927.1	445.6	27.31	2.70	26.95	19	0.51	82.1	1.8
570	466.0	471.8	26.74	2.75	26.50	23	0.14	−73.8	5.1
626	922.0	505.1	24.91	2.76	25.38	57	0.22	−62.5	26.5
704	986.9	545.2	24.91	2.78	25.66	102	0.31	83.8	13.0
725	961.6	562.1	26.83	2.77	26.48	19	0.33	−58.2	21.8
735	963.4	566.4	27.06	2.72	26.65	16	0.82	−61.4	17.9
782	129.3	597.6	25.41	2.77	25.92	44	0.93	56.5	22.0
912	552.4	710.4	24.12	2.76	24.63	61	0.62	−17.9	33.2
945	813.2	735.5	26.04	2.76	26.00	46	0.36	−64.3	23.5
965	347.9	750.4	26.00	2.79	25.97	42	0.35	−82.1	51.6
979	642.7	762.7	24.09	2.71	24.92	151	0.14	−8.9	1.8
1022	101.7	808.2	23.99	2.75	24.82	136	0.33	85.1	26.4
1029	493.6	815.6	25.17	2.80	25.80	83	0.44	4.4	15.8
1032	429.3	817.0	26.60	2.78	26.41	30	0.34	14.6	15.0
1175	833.7	980.8	27.31	2.75	26.89	14	0.33	−32.6	7.7

NOTES.—Data for the 23 objects with color $2.7 \leq B-I \leq 2.8$. Col. (1) gives their number in our FOCAS catalog, cols. (2) and (3) give their center coordinates in pixels, col. (4) gives their B magnitude, col. (5) their $B-I$ color, col. (6) their central brightness in B, col. (7) their area in pixels, col. (8) their ϵ from eq. (2.1), col. (9) their orientation ϕ in degrees, and col. (10) their axis-to-tangent angle η in degrees. For reference, the coordinates of the four bright central galaxies are (565.5, 520.5), (589, 506.5), (607, 520), and (633, 484). The scale is 1 pixel = 0".206.

Objects" (TARO). Given our data, we do not have the means to distinguish between the TARO and the foreground contamination.

In addition to our B and I images we have also examined the *Hubble Space Telescope* images of Cl 0024+1654 obtained by A. Dressler and collaborators in 1992, which have become available in the *HST* Archive. The *HST* images cover a smaller part of the cluster than the CFHT images, but all our $2.7 \leq B-I \leq 2.8$ objects which are within the *HST* field are easily identifiable. Unfortunately, the deconvolution procedure of the image before the repairs of the *HST* optics and the lack of the "shift-and-add" procedure (Tyson 1988) made these images inferior to our B and I images as regards the photometry and shapes of faint objects, despite good detection.

If the TARO are normal galaxies at a redshift higher than the typical redshift of galaxies in the catalog with a similar color, we can expect the diminution of brightness with redshift to bias their areas to be typically smaller than the areas of objects with adjacent colors. We find that the average area of the $2.7 \leq B-V \leq 2.8$ objects, $\bar{A} = 31.4 \pm 5.2$ pixels, is indeed smaller than the average area of the objects in $B-I$ intervals (2.5, 2.7) and (2.8, 3.0) taken together, $\bar{A} = 46.6 \pm 3.3$ pixels, where the errors are assigned by taking the measured dispersion and dividing it by $N^{1/2}$.

The most outstanding feature of the TARO is their very narrow, $\Delta(B-I) \leq 0.1$ mag, spread in color. Their color lies roughly in a "window" between the typical colors of ellipticals and spirals/irregulars of Cl 0024 + 1654, but from the distribution of all objects in $B-I$ we see that this fact alone does not account for the thinness of the red spike. If different TARO had quite different redshifts, the $2.7 \leq B-I \leq 2.8$ color range would imply a power-law spectrum $\nu F_\nu(Wm^{-2}) \propto \nu^{-2.2\pm0.1}$ and a new type of high-redshift extended objects heretofore unknown. We are thus led to a hypothesis that most of the TARO have approximately the same redshift, z_r, and a very narrow intrinsic distribution in color.

Natural candidates for such objects are elliptical galaxies, for two reasons. One is that they tend to have smaller ellipticities in projection than spirals (e.g., Lambas, Maddox, & Loveday 1992), so that their images have a higher response to the distortion by a gravitational lens. Another is that the redshift-color correlation seems to be much more narrow for ellipticals than for spirals, as for example the brighter galaxies in the Coma cluster have a ~ 0.2 mag width of their ditribution in the $b-r$ color (Mazure et al. 1988; see also Aragón-Salamanca et al. 1993 for distant clusters and references to recent literature). A natural explanation for the TARO being at the same redshift is that they are physically associated and belong to a cluster of galaxies.

It is practically impossible to have a good guess on the redshift of TARO from the single $B-I$ color and from the central brightness (the latter is $\sim 6 \pm 1$ mag fainter than that of the brightest galaxies in Cl 0024+1654), as we do not know the true evolutionary history of galaxies. This history can affect very much the K-corrections and the redshift fitting $B-I = 2.75$. As a reference possibility, we note that the color and brightness of TARO are consistent with $z_r \sim 1.8$, if we assume an extreme scenario in which ellipticals form at $z \sim 5$ and do not evolve (for an Einstein–de Sitter universe [$q_0 = 1/2$], and a Hubble constant $h = 1/2$ in units of 100 km s^{-1} Mpc^{-1}) (R. Pelló 1994, private communication). If there is evolution, z_r would tend to decrease.

We also note a possible speculation that the color of TARO is caused by a Lyα emission line redshifted into the I_{7800} filter bandpass. This would place TARO at $z_r \approx 5.5$ and require them to have Lyα active regions of size $\sim$ a few kpc, and

luminosities of 10^{43}–$10^{44.5}$ ergs s^{-1} h^{-2} in the I_{7800} band (assuming an EdS universe), compatible with what is expected for primordial galaxies (e.g., Parks, Collins, & Joseph 1994 and references therein). This may not necessarily be a too exotic hypothesis as there is some evidence on extended Lyα-emitting objects at high redshift (cf. Djorgovski et al. 1985; Schneider et al. 1987; Hu et al. 1991). However, this speculation explains neither the narrow color range of the red spike nor why these galaxies are detected in B at all, as the B filter would then be beyond the Lyman limit. It also may conflict with common theories of galaxy formation.

Given the uncertainty of guesses on the TARO redshift, Kassiola, Kovner, & Dantel-Fort (1994, Paper III) investigated whether there are bounds on z_r from the constraints known to date on the gravitational lensing properties of Cl 0024+1654. Two hypotheses were considered: (1) that the TARO are all single images at $z_r = 5.5$, and (2) that some of the TARO can be matched as images of the same source, in a lens model that simultaneously reproduces the Triple Arc at $z_{ta} = 1$. Neither hypothesis could be excluded. In the latter, two pairs of red objects were matched, 221–979 and 305–1029, with redshift $z_r = 5.5$. Thus, given the present-day data, it is not possible to rule out the high-redshift hypothesis for the TARO from gravitational lensing arguments alone.

4. CONCLUSION

As expected, selection for blue color does indeed increase the signal-to-noise ratio in statistics of distortions of background objects by clusters of galaxies. Much more surprising is the discovery of the red spike of tangential alignment at $2.7 \leq B-I \leq 2.8$. We recapitulate our main points on the latter.

First, the 10^{-6} probability for the red spike to occur by chance makes us think that it is real, despite the 40 steps in the histogram and the choice of advantageous thresholds on the area and central brightness in our statistics. With disadvantageous thresholds the probability would still be $\lesssim 10^{-4.5}$. Second, our favorite hypothesis to account for this spike is that it is caused by elliptical galaxies belonging to a cluster at redshift $z_r \lesssim 1.8$, or perhaps by a group of young galaxies created all nearly at the same time.

A more speculative possibility is that the tangentially aligned red objects (TARO) can be primordial galaxies at $z_r \sim 5.5$ and owe their color to a Lyα emission line redshifted into the I_{7800} bandpass. The constraints available to data on the lensing properties of Cl 0024+1654 do not rule out very high redshift for the TARO. However, this hypothesis does not explain their narrow color range and why they are detected in B at all.

Finally, we note that all of our $2.7 \leq B-I \leq 2.8$ objects that were in the field of the *HST* images of Cl 0024+1654 are easily seen in these images. Deep photometry accompanied by the "shift-and-add" technique would make the repaired *HST* the best tool to resolve the nature of these objects.

Besides the TARO, there is a suggestion of another possible isolated spike of alignment at $1.7 \leq B-I \leq 1.9$, in the fine histograms of Figure 1. However its probability to occur by chance is only $\approx 10^{-2.7}$ and it is close to the broad blue alignment signal.

Whatever the redshift of the TARO, it seems clear that the use of color selection and statistical tangential alignment enables us to discover very distant clusters or groups of galaxies. Essentially, in what we have described, Cl 0024+1654 played a role of a combination of a zoom and a "distortion filter" attached to the CFHT. We believe that very deep observations of clusters of galaxies should routinely be checked for tangential alignment and its dependence on color, in order to identify possible groupings of distant objects behind the cluster.

We thank M. Dantel-Fort for her help in data processing, D. Fraix-Burnet and R. Pelló for their help in obtaining and processing the *HST* images, H. Bonnet and G. Soucail for helpful advice, M. Bartelmann, P. Schneider, S. Seitz, and J. Wambsganss for moral support, and the referee for helpful suggestions. A. K. acknowledges financial support from the program "Human Capital and Mobility" of the E.E.C., and I. K. acknowledges support by the sabbatical funds from the Weizmann Institute of Science (Israel).

REFERENCES

Aragón Salamanka, A., Ellis, R. S., Couch, W. J., & Carter, D. 1993, MNRAS, 262, 764
Blandford, R. D., & Narayan, R. 1992, ARA&A, 30, 311
Bonnet, H., Mellier, Y., & Fort, B. 1994, 427, L83
Djorgovski, S., Spinrad, H., McCarthy, P., & Strauss, M. A. 1985, ApJ, 299, L1
Fort, B. 1992, in Gravitational Lenses, ed. R. Kayser, T. Schramm, & L. Nieser (Berlin: Springer), 267
Hu, E. M., Songalia, A., Cowie, L. L., & Stockton, A. 1991, ApJ, 368, 28
Jarvis, J. F., & Tyson, J. A. 1981, AJ, 86, 476
Kassiola, A., Kovner, I., & Dantel-Fort, M. 1994, MNRAS (Raper III), submitted
Kassiola, A., Kovner, I., & Fort, B. 1992, ApJ, 400, 41 (Paper I)
Kendall, M., & Stuart, A. 1977, Distribution Theory (4th ed.; London: Charles Griffin), vol. 1, ch. 11, ex. 11.14, p. 278
Lambas, D. G., Maddox, S. J., & Loveday, J. 1992, MNRAS, 258, 404
Mazure, A., Proust, D., Mathez, G., & Mellier, Y. 1988, A&AS, 76, 339
Parkes, I. M., Collins, C. A., & Joseph, R. D. 1994, MNRAS, 266, 983
Pelló, R., Le Borgne, J.-F., Sanahuja, B., Mathez, G., & Fort, B. 1992, A&A, 266, 6
Schneider, D. P., Gunn, J. E., Turner, E. L., Lawrence, C. R., Hewitt, J. N., Schmidt, M., & Burke, B. F. 1986, AJ, 91, 991
Schneider, P., Ehlers, J., & Falco, E. E. 1992, Gravitational Lenses (Berlin: Springer)
Tyson, J. A. 1988, AJ, 96, 1
Tyson, J. A., Valdes, F., Jarvis, J. F., & Mills, A. P., 1984, ApJ, 281, L59
Valdes, F., Tyson, J. A., & Jarvis, J. F. 1983, ApJ, 271, 431
Webster, R. L. 1985, MNRAS, 213, 871